

## Waterbomb origami as energy harvester

Guilherme V. Rodrigues <sup>1</sup>, Marcelo A. Savi <sup>2</sup>

<sup>1</sup> Universidade Federal do Rio de Janeiro, guilherme\_@live.co.uk

<sup>2</sup> Universidade Federal do Rio de Janeiro, savi@mecanica.coppe.ufrj.br

*Abstract: Origami has inspired several fields of engineering, motivating the creation of novel adaptive and morphing structures. Recently, the folding along the crease pattern of origami-inspired mechanisms has been harnessed in energy harvesting. This paper describes the use of a waterbomb origami as a potential energy harvester. Bistability inherent in the waterbomb base origami can be utilized to increase the bandwidth of its frequency response. A dynamical model is proposed and performance of the origami is investigated under external excitations.*

**Keywords:** origami, vibration, energy harvesting, bistability

### INTRODUCTION

Origami is a Japanese art practiced for hundreds of years but only recently it has been gaining attention for its potential to provide novel solutions to engineering systems. The origami-inspired structures have been applied considering different folding patterns as innovative designs (Hernandez *et al.*, 2014). Fonseca *et al.* (2022) presented a general review of origami-inspired systems and structures. Examples of applications have been found in versatile architectures (Sorguç *et al.*, 2009), aerospace-based systems (Zirbel *et al.*, 2013), surgical tools (Mohanta *et al.*, 2019), miniature robots (Miyashita *et al.*, 2015) energy absorption (Song *et al.*, 2012), among others (Meloni *et al.*, 2021).

Origami-inspired structures are versatile since they are able to present stiffness variations and folding/unfolding behaviors. One of the attractive features of these structures is their geometrically driven multistability, which has been applied in metamaterials with programmable reconfiguration of shape and bulk properties (Overvelde *et al.*, 2016).

The multistability associated with buckling in origami-inspired structures have been of interest for energy harvesting applications. A rapid snapping action between structure stable states subjected to dynamical loading implies a broadband response. In addition to the strong nonlinear characteristics of origami-inspired structures, a sudden geometric or stiffness variation can be harnessed for broadband energy harvesting purposes.

One of the most well-known origami pattern is the waterbomb pattern (Ma and You, 2014), which has been employed to build foldable cylinders as stent grafts (Kuribayashi *et al.*, 2016), worm robots (Onal *et al.*, 2012) and deformable robot wheels (Lee *et al.*, 2013). The waterbomb pattern is of interest due to its simple topology and scalability, together with an interesting kinetic behavior that allows it to behave as one- or two-way bistable mechanism (Hanna *et al.*, 2014).

This work deals with vibration energy harvesting of a six-crease waterbomb base origami. The bistability inherent in this pattern is profited to increase the bandwidth of its frequency response enhancing the energy harvesting capacity.

### Waterbomb origami: a bistable mechanism

The waterbomb base origami has a folding pattern that has been used as a foundation for complex origami designs. There are two types of waterbomb pattern: the six-crease and the eight-crease (Chen *et al.*, 2016). The six-crease waterbomb pattern proved to be useful in a variety of applications because its tessellations range from a flat-foldable surface to a deformable tube (Fonseca *et al.*, 2019), Fig. (1).

A spring-like behavior can be assigned to the waterbomb origami and two equilibrium states are settled, Fig. (2). It is known that its force-deflection curve is nonlinear, actuating as a nonlinear spring. When its motion is between the first stable equilibrium state and the unstable equilibrium state, it is unimodal despite its nonlinearity. Nevertheless, a sufficiently large input displacement promotes a transition from the first stable equilibrium state, through the unstable equilibrium state, to the second stable equilibrium state.

This work focuses on the six-crease waterbomb pattern and its kinematics is presented in the sequel. Two independent parameters define the pattern, length  $L$  and sector angle  $\alpha$ .

Origami-inspired structures are modeled according to their mechanical behavior (Fonseca *et al.*, 2022). Considering the rigid origami theory, deformations of structural components does not occur during the deployment process, and the panels remain flat at any condition (Filipov *et al.*, 2017). Under this assumption, it is known that the waterbomb base has 3-degrees of freedom (Fonseca *et al.*, 2021). However, it can be reduced to a single-degree of freedom if symmetries are considered (Rodrigues and Savi., 2021).

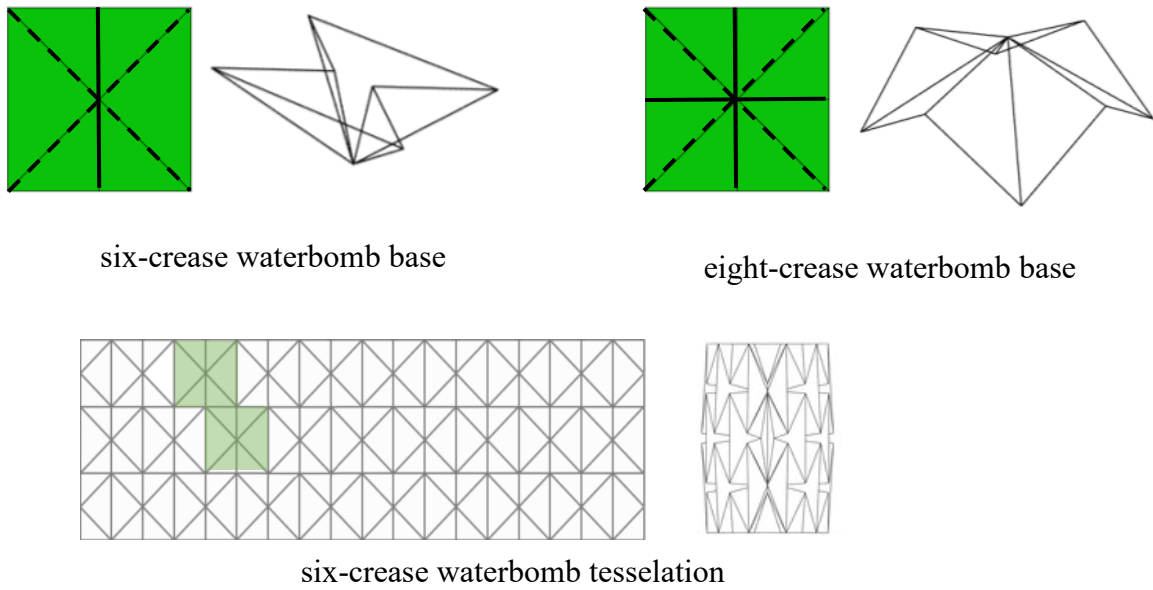


**Figure 1 – Waterbomb pattern: six-crease base and eight-crease base. Tessellation of a six-crease waterbomb base form a cylindrical deformable structure.**

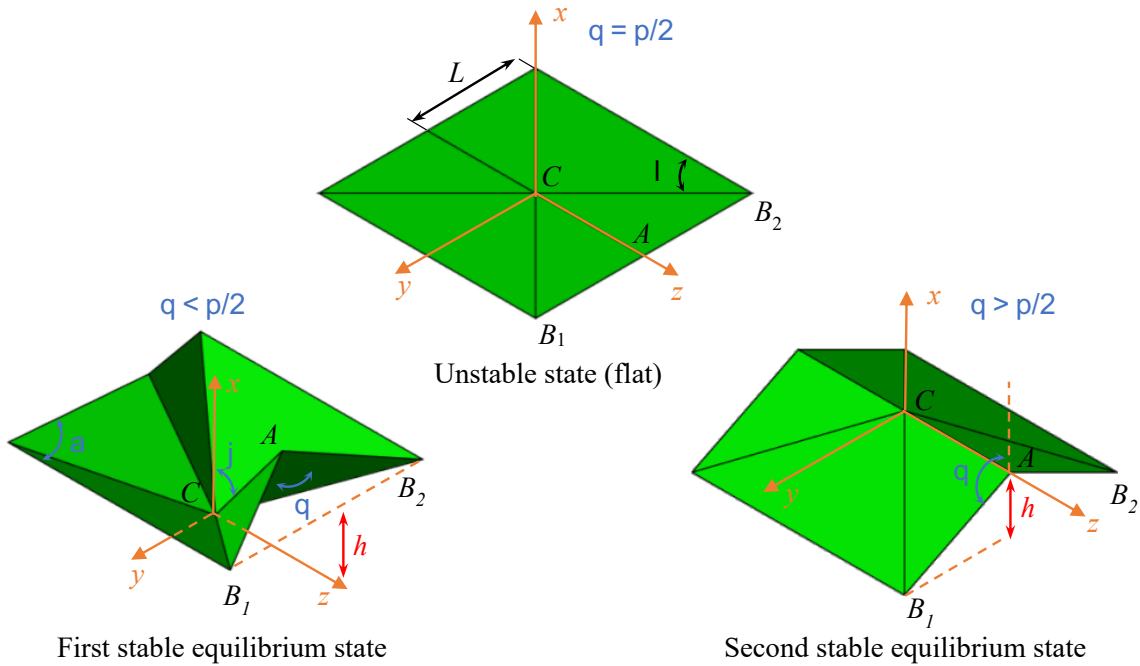


**Figure 2 – Equilibrium states of the six-crease waterbomb base.**

By considering the angles presented in Fig. (2), the rigid origami theory implies a constraint that furnishes the following set of equations:

$$\cos(\theta) \cos(\varphi) \tan(\lambda) + \sin(\varphi) = 1 \tag{1-a}$$

$$2 \tan(\lambda) \cos \alpha + \tan(\lambda) \sin(2\varphi) \cos \theta - \cos(2\varphi) = 1 \tag{1-b}$$

The relations defined in Eq. (1) are veracious from the first state ( $\theta < \pi/2$ ) up to the flat state ( $\theta = \pi/2$ ). This is the first stage of deployment. The second stage is performed with  $\varphi$  remaining constant and equal to  $\pi/2$  while the angle  $\theta$  varies. Aiming to have the angle deployment between the stages, the angle  $\theta$  is redefined as in Fig. (2). Therefore,  $\theta >$

$\pi/2$  characterizes the second stage. Based on that, two stable equilibrium points are established, one in each stage of deployment.

## Origami-based energy harvesting

Dynamical folding and unfolding of origami-inspired mechanism are responsible to originate large angle change between its adjacent facets, which is useful to convert a portion of ambient mechanical energy into electricity. Therefore, multistable origami-inspired mechanisms subjected to external vibrations can experience significant geometric change serving as mechanical devices to harvest vibration energy in a relatively broadband frequency.

An origami-based energy harvester can be formed by attaching piezoelectric films over the folds. Power from the ambient vibration is harnessed by localized deformation of the piezoelectric films over the folds that directs the motion of charges towards the electrodes. For a bistable origami, snap-through behavior gives rise to its broadband frequency response, which is desirable a more effective energy harvesting.

Some recent works has exploited origami-inspired mechanism as energy harvesters. Tao *et al.* (2019) designed an origami-inspired TENG (triboelectric nanogenerators) with great potential for biomechanical and ocean wave energy harvesting. Wang *et al.* (2020) designed a similar device that can switch from bidimensional to three-dimensional state, which improve the output performance of TENG and can be successfully integrated into floors and smart shoes. Miranda *et al.* (2020) investigated origami-inspired sunscreens equipped with piezoelectric cables under the action of wind forces. Chung *et al.* (2021) developed a triangular cylinder origami-based hybrid generator composed by a vertical contact separation TENG on the surface and PENG (piezoelectric nanogenerators) on the inner hinges, which can harvest mechanical energy from each motion.

Ngo *et al.* (2022) proposed a vibration energy harvester based on an eight-crease waterbomb base through piezoelectric energy conversion, creating a device with excellent deformability and flexibility. In this paper, a six-crease waterbomb base is considered instead. Since the tessellation of the six-crease waterbomb base generates a foldable cylindrical structure, which does not happen with the eight-crease waterbomb base, this work is a novel strategy.

## MATHEMATICAL MODEL

Waterbomb origami is modeled as a single-degree of freedom mechanism. According to the rigid origami theory, the facets are assumed to be rigid. The creases are assumed to be elastic hinges represented by linear torsional stiffness. Based on that, it is possible to write the total potential energy of the waterbomb pattern:

$$\Psi = \frac{1}{2} [2k_{\theta}(2\theta - 2\theta_0)^2 + 4k_{\alpha}(\alpha - \alpha_0)^2] \quad (2)$$

where  $k_{\theta}$  and  $k_{\alpha}$  are torsional stiffness and  $\theta_0$  and  $\alpha_0$  are the angles corresponding to the stress-free stable states.

The kinematics related to Eq. (1) provides a direct relation between the angles  $\alpha$  and  $\theta$ . The potential energy  $\Psi$  as a function of  $\theta$  is presented in Fig. (3) for different set of values. Its double-well characteristics is due to the transition between the stages, presenting a large influence to the energy harvesting process.

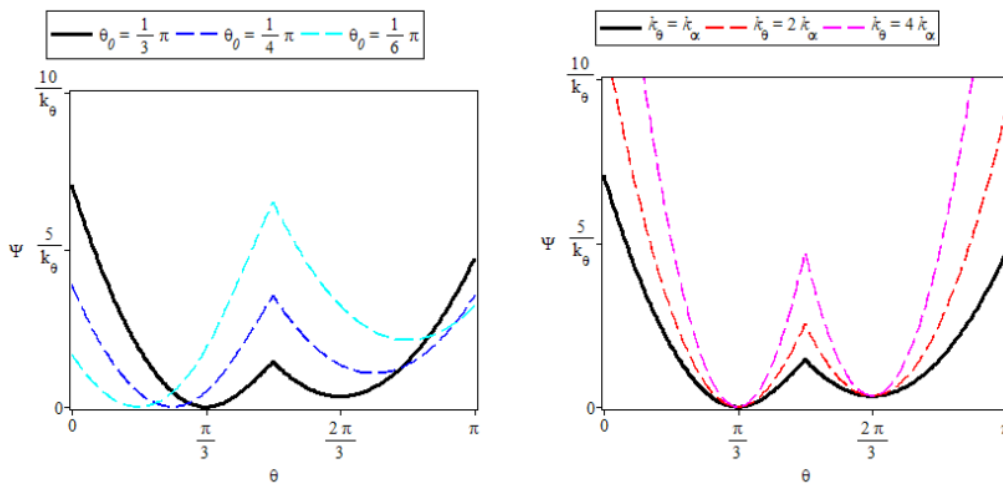


**Figure 3 – Double-well potential energy of the six-crease waterbomb origami. In the left, it is considered different equilibrium angles. In the right, it is considered different stiffness on the creases.**

The deployment of the waterbomb base origami can be treated by considering the height  $h = L \cos \theta$  (Fig. 2). Thus, force-displacement relation can be obtained by the derivative of the potential energy  $\Psi$  with respect to the height  $h$ , given by the following equation:

$$F = \frac{d\Psi}{dh} = \frac{d\Psi}{d\theta} \left( \frac{dh}{d\theta} \right)^{-1} \quad (3)$$

A lumped mass in the central vertex of the waterbomb base origami that is initially at the position  $h_0$ , corresponding to the initial angle  $\theta_0$ , is considered. Besides, a harmonic base excitation  $f = f_0 \sin(\omega t)$  is assumed. By considering that the deployment of the waterbomb origami is described by a displacement  $u = h - h_0$ , the equation of motion is as follows:

$$\begin{cases} m\ddot{u} + c\dot{u} + F(u) - K_V V = -m\ddot{f} \\ \dot{V} = -K_C \dot{u} - V/R_L C \end{cases} \quad (4)$$

where  $m$  denotes a lumped mass,  $c$  is a viscous damping coefficient,  $K_V$  and  $K_C$  are coefficients responsible for electromechanical coupling properties of the piezoelectric element,  $V$  is the voltage output,  $R_L$  is the load resistance and  $C$  is the capacitance of the piezoelectric element (Paula *et al.*, 2015; Costa *et al.*, 2021).

The dimensionless form of the equations of motion is given by:

$$\begin{cases} \ddot{x} = -\xi \dot{x} - \bar{F}(x) + \chi V - \gamma \sin(\Omega\tau) \\ \dot{V} = -\kappa \dot{x} - \rho V \end{cases} \quad (5)$$

where  $x = u/L$  is the dimensionless displacement,  $\tau$  represents a dimensionless time.

The performance of the piezoelectric structure is evaluated by the RMS (root mean square) power and by the efficiency in power conversion:

$$\eta = \frac{P_{out}}{P_{in}} = \frac{\sqrt{\frac{1}{\tau} \int_0^\tau \rho \dot{V}^2 d\tau}}{\sqrt{\frac{1}{\tau} \int_0^\tau \dot{x} \gamma \sin(\Omega\tau) d\tau}} \quad (6)$$

where  $P_{in}$  and  $P_{out}$  are the overall input and output power considering the RMS of the instantaneous mechanical power ( $P_m$ ) and instantaneous electrical power ( $P_e$ ) respectively.

## NUMERICAL SIMULATIONS

Equations of motion are solved by employing the fourth-order Runge–Kutta method considering a period of time long enough to ensure that transients have elapsed and a steady-state solution is achieved. Table 1 presents parameter of the origami energy harvester.

**Table 1 – Parameters of the origami energy harvester.**

Parameter	Value
Length $L$ (mm)	60.0
Sector angle $\lambda$ (degree)	45.0
Stiffness $k_\theta = k_\alpha$ (N m rad <sup>-1</sup> )	0.0010
Initial height $h_0$ (mm)	30.0
Lumped mass $m$ (g)	50.0
Damping coefficient $c$ (N s m <sup>-1</sup> )	0.50
Piezoelectric coefficient coupling $\chi$	0.05
Piezoelectric coefficient coupling $\kappa$	0.50
Piezoelectric parameter $\rho$	0.05

Bistable structures present the most interesting behavior for energy harvesting purposes. Fig (4) presents the dynamical response of the waterbomb origami under an external amplitude force  $f_0 = 1$  mm. Two different but close initial conditions are considered,  $u_0 = 30$  mm and  $u_0 = 31$  mm. Accordingly with these initial conditions, despite the small difference, the waterbomb base oscillates around one or other stable equilibrium point, at  $u = 0$  and  $u = -60$  mm.

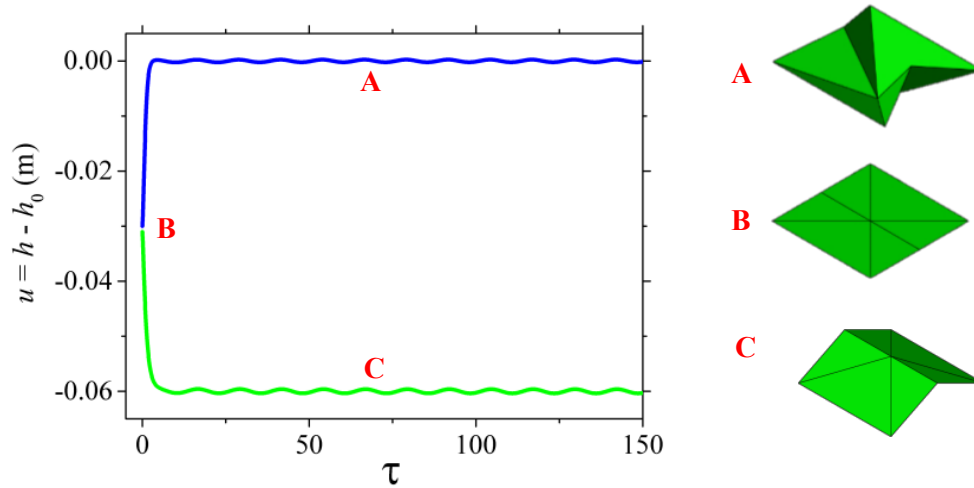


Figure 4 – Equilibrium points of the waterbomb origami.

Interwell oscillations enlarge the bandwidth of power output of the energy harvester when compared to the case when the response is confined to intrawell oscillation, restricted to a single well. The goal is to define suitable excitations that lead to enhanced energy harvesting. Three cases are presented in the sequel (Fig. 5 to Fig. 7): oscillation around equilibrium point A (Fig. 5); oscillation around equilibrium point C (Fig. 6); and oscillation around both equilibrium points (Fig. 7). The efficiency is calculated for each case and the external excitation frequency is adopted to be  $\omega = 5$  Hz.

By considering  $u_0 = 0$ , the system response is presented in Fig. (5) showing displacement, instantaneous power and efficiency. The central vertex of the waterbomb origami oscillates with an amplitude around 0.2 mm, and the RMS mechanical power is 26.9 nanowatts while the RMS electrical power is 4.2 nanowatts, providing an efficiency of 15.6%.

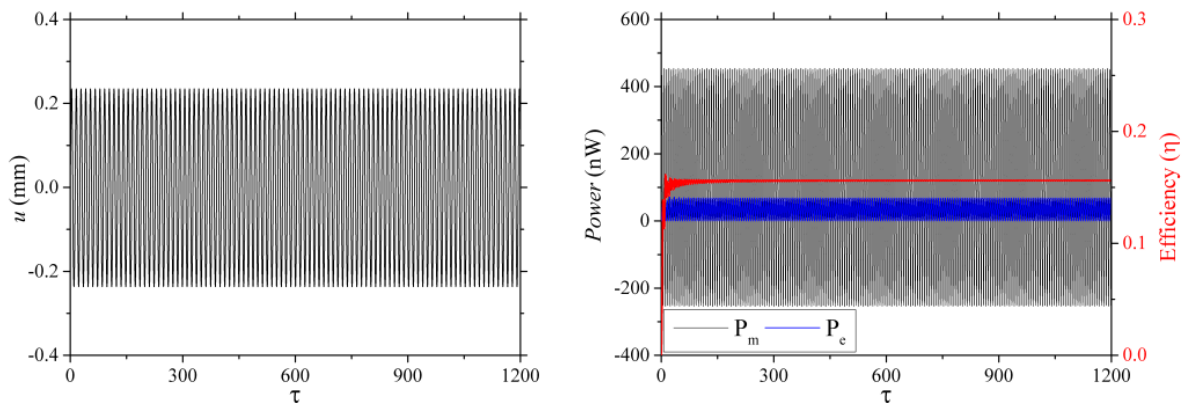


Figure 5 – Dynamical response around equilibrium point A and its power generated and efficiency.

By considering an initial condition related to the other equilibrium point,  $u_0 = -60$  mm, the amplitude of the response is close to 0.4 mm (Fig. 6), almost the double of the previous case. The RMS mechanical power is 48.0 nanowatts and the RMS electrical power is 11.0 nanowatts. When compared to the previous case, it is noticeable that the increase of the electrical power is more significant than the increase of the mechanical power. The efficiency is now 22.9%. Despite the same conditions of external excitations, these two cases present different behaviors due to the geometry of the waterbomb origami.

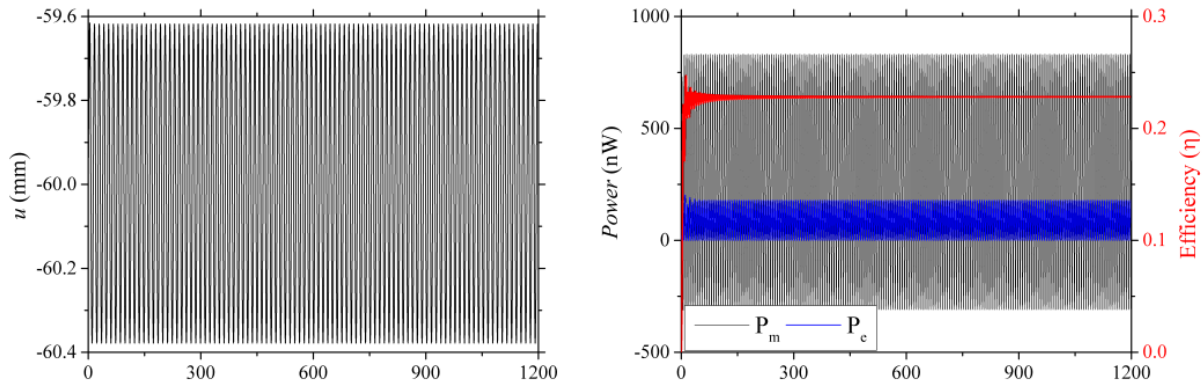


Figure 6 – Dynamical response around equilibrium point C and its power generated and efficiency.

By considering an increase of the external amplitude from  $f_0 = 1$  mm to  $f_0 = 90$  mm, the system response is presented in Fig. 7. The central vertex oscillates around both equilibrium points A and C, which characterizes an interwell oscillation. The amplitude of oscillation is around 45mm and the power generated is in the order of milliwatts. Despite these higher values, the efficiency does not increase, being about 16.7%. The RMS mechanical power is 98.4 milliwatts while the RMS electrical power is 16.4 milliwatts.

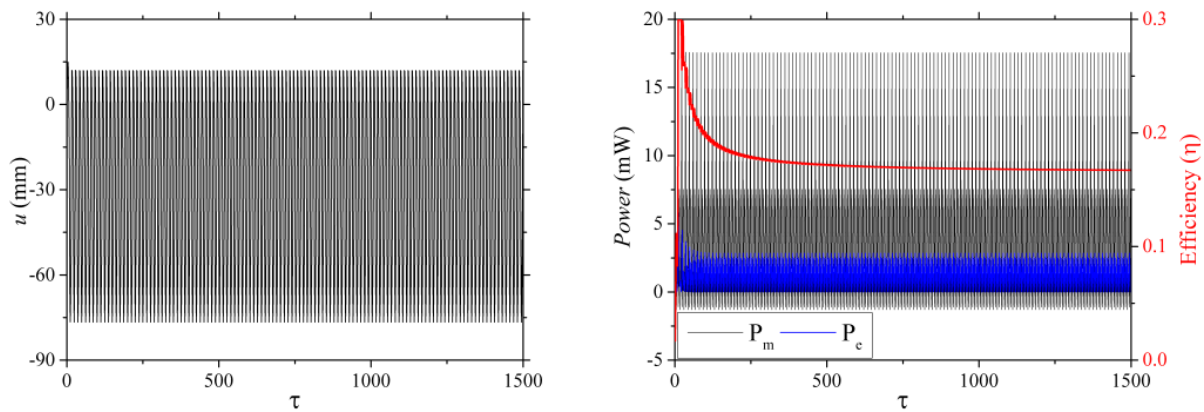


Figure 7 – Dynamical response around equilibrium points A and C (interwell oscillation).

Thus, bistable system can improve the provided power, however, this does not necessarily happen when it oscillates around both stable equilibrium points.

## CONCLUSIONS

A waterbomb origami dynamical model is proposed for energy harvesting purpose. The origami-inspired structure is integrated with piezoelectric films to create a device with excellent deformability and flexibility. The bistability of this structure enhance the mechanical low frequency energy harvesting. The performance of the waterbomb origami has been investigated under different conditions showing that this application has an interesting potential to enhance energy harvesting capacity.

## ACKNOWLEDGMENTS

The authors would like to acknowledge the support of the Brazilian Research Agencies CNPq, CAPES and FAPERJ.

## REFERENCES

- Chen, Y., Feng, H., Ma, J., Peng, R., & You, Z. (2016). Symmetric waterbomb origami. *Proceedings of the Royal Society A: Mathematical, Physical and Engineering Sciences*, 472(2190), 20150846.
- Chung, J., Song, M., Chung, S. H., Choi, W., Lee, S., Lin, Z. H., Hong, J. & Lee, S. (2021). Triangulated Cylinder Origami-Based Piezoelectric/Triboelectric Hybrid Generator to Harvest Coupled Axial and Rotational Motion. *Research*, 2021, 7248579.
- Costa, L. G., Monteiro, L. L. D. S., Pacheco, P. M. C. L., & Savi, M. A. (2021). A parametric analysis of the nonlinear dynamics of bistable vibration-based piezoelectric energy harvesters. *Journal of Intelligent Material Systems and Structures*, 32(7), 699-723.

- Filipov, E. T., Liu, K., Tachi, T., Schenk, M., & Paulino, G. H. (2017). Bar and hinge models for scalable analysis of origami. *International Journal of Solids and Structures*, 124, 26–45.
- Fonseca, L. M., Rodrigues, G. V., & Savi, M. A. (2022). An Overview of the Mechanical Description of Origami-Inspired Systems and Structures. *International Journal of Mechanical Sciences*, 107316.
- Fonseca, L. M., Rodrigues, G. V., Savi, M. A., & Paiva, A. (2019). Nonlinear dynamics of an origami wheel with shape memory alloy actuators. *Chaos, Solitons & Fractals*, 122, 245-261.
- Fonseca, L. M., Savi, M. A., (2021). On the symmetries of the Origami Waterbomb Pattern: Kinematics and Mechanical Investigations. *Meccanica* (2021).
- Hanna, B. H., Lund, J. M., Lang, R. J., Magleby, S. P., & Howell, L. L. (2014). Waterbomb base: a symmetric single-vertex bistable origami mechanism. *Smart Materials and Structures*, 23(9), 094009.
- Hernandez, E. A., Hartl, D. J., Malak Jr, R. J., & Lagoudas, D. C. (2014). Origami-inspired active structures: a synthesis and review. *Smart Materials and Structures*, 23(9), 094001.
- Kuribayashi, K., Tsuchiya, K., You, Z., Tomus, D., Umemoto, M., Ito, T., & Sasaki, M. (2006). Self-deployable origami stent grafts as a biomedical application of Ni-rich TiNi shape memory alloy foil. *Materials Science and Engineering: A*, 419(1-2), 131-137.
- Lee, D. Y., Kim, J. S., Kim, S. R., Koh, J. S., & Cho, K. J. (2013b). The deformable wheel robot using magic-ball origami structure. In *International Design Engineering Technical Conferences and Computers and Information in Engineering Conference*, 55942, V06BT07A040. American Society of Mechanical Engineers.
- Ma, J., & You, Z. (2014, August). Modelling of the waterbomb origami pattern and its applications. In *International Design Engineering Technical Conferences and Computers and Information in Engineering Conference* (Vol. 46377, p. V05BT08A047). American Society of Mechanical Engineers.
- Meloni, M., Cai, J., Zhang, Q., Sang - Hoon Lee, D., Li, M., Ma, R., Parashkevov, T. E. & Feng, J. (2021). Engineering Origami: A comprehensive review of recent applications, design methods, and tools. *Advanced Science*, 2000636.
- Miranda, R., Babilio, E., Singh, N., Santos, F., & Fraternali, F. (2020). Mechanics of smart origami sunscreens with energy harvesting ability. *Mechanics Research Communications*, 105, 103503.
- Miyashita, S., Guitron, S., Ludersdorfer, M., Sung, C. R., & Rus, D. (2015). An untethered miniature origami robot that self-folds, walks, swims, and degrades. In *2015 IEEE International Conference on Robotics and Automation (ICRA)*, 1490-1496. IEEE.
- Mohanta, D., Mohapatra, S., Khuntia, S., Sahoo, S., & Rauta, P. R. (2019). Origami-Engineered Structures and Their Biomedical Applications. In *Nanotechnology in Biology and Medicine*, 167-173. CRC Press.
- Ngo, T. H., Chi, I., Chau, M. Q., & Wang, D. A. (2022). An Energy Harvester Based on a Bistable Origami Mechanism. *International Journal of Precision Engineering and Manufacturing*, 1-14.
- Onal, C. D., Wood, R. J., & Rus, D. (2012). An origami-inspired approach to worm robots. *IEEE/ASME Transactions on Mechatronics*, 18(2), 430-438.
- Overvelde, J. T., De Jong, T. A., Shevchenko, Y., Becerra, S. A., Whitesides, G. M., Weaver, J. C., Hoberman, C. & Bertoldi, K. (2016). A three-dimensional actuated origami-inspired transformable metamaterial with multiple degrees of freedom. *Nature communications*, 7(1), 1-8.
- Paula, A. S., Inman, D. J., & Savi, M. A. (2015). Energy harvesting in a nonlinear piezomagnetoelastic beam subjected to random excitation. *Mechanical Systems and Signal Processing*, 54, 405-416.
- Rodrigues, G. V., & Savi, M. A. (2021). Reduced-Order Model Description of Origami Stent Built with Waterbomb Pattern. *International Journal of Applied Mechanics*, 13(2), 2150016.
- Song, J., Chen, Y., & Lu, G. (2012). Axial crushing of thin-walled structures with origami patterns. *Thin-Walled Structures*, 54, 65-71.
- Sorguç, A. G., Hagiwara, I., & Selcuk, S. E. M. R. A. (2009). Origamics in architecture: a medium of inquiry for design in architecture. *Metu Jfa*, 2, 235-247.
- Tao, K., Yi, H., Yang, Y., Chang, H., Wu, J., Tang, L., Yang, Z., Wang, N., Hu, L., Fu, Y., Miao, J. & Yuan, W. (2019). Origami-inspired electret-based triboelectric generator for biomechanical and ocean wave energy harvesting. *Nano Energy*, 67, 104197.
- Wang, Y., Wu, Y., Liu, Q., Wang, X., Cao, J., Cheng, G., Zhang, Z., Ding, J. & Li, K. (2020). Origami triboelectric nanogenerator with double-helical structure for environmental energy harvesting. *Energy*, 212, 118462.
- Zirbel, S. A., Lang, R. J., Thomson, M. W., Sigel, D. A., Walkemeyer, P. E., Trease, B. P., Magleby, S. P. & Howell, L. L. (2013). Accommodating thickness in origami-based deployable arrays. *Journal of Mechanical Design*, 135(11).

## RESPONSIBILITY NOTICE

The authors are the only parties responsible for the printed material included in this paper.